How to cite: *Angew. Chem. Int. Ed.* **2022**, *61*, e202113406
International Edition: doi.org/10.1002/anie.202113406
German Edition: doi.org/10.1002/ange.202113406

Analytical Methods

Quantifying Intracellular Single Vesicular Catecholamine Concentration with Open Carbon Nanopipettes to Unveil the Effect of L-DOPA on Vesicular Structure

*Keke Hu[+], Kim Long Le Vo[+], Amir Hatamie, and Andrew G. Ewing**

Abstract: *Understanding the regulatory mechanisms of exocytosis is essential for uncovering the pathologies of neuronal disorders and developing related pharmaceuticals. In this work intracellular vesicle impact electrochemical cytometry (IVIEC) measurements with different-sized (50–500 nm radius) open carbon nanopipettes (CNPs) were performed to quantify the vesicular content and release kinetics of specific vesicle populations grouped by orifice sizes. Intracellular vesicles with radius below 100 nm were captured and narrowed between 50 and 100 nm. On the basis of this, single vesicular catecholamine concentrations in the intracellular environment were quantified as 0.23–1.1 M. Our results with L-3,4-dihydroxyphenylalanine (L-DOPA)-exposure indicate that L-DOPA regulates exocytosis by increasing the dense core size and vesicular content while catecholamine concentrations did not show obvious alterations. These were all achieved simultaneously and relatively noninvasively with open CNPs.*

Neuronal communication is mediated by nanometer-sized vesicles that are responsible for carrying and releasing the signaling transmitters through a process called exocytosis. It is crucial for the survival of the organisms and dysfunctional communication is implicated in the pathologies of many neurodegenerative diseases and memory disorders. Exocytosis is a tightly regulated biological activity involving both small synaptic vesicles (SSVs) and large dense core vesicles (LDCVs), and the regulatory mechanisms have been studied extensively in molecular biology, biochemistry and neuroscience with model cells that contain LDCVs.[1] In LDCVs, the dense core is primarily made up of aggregated chromogranins with bound transmitters surrounded by a halo with freely moving transmitters.[2] A number of techniques including electrochemical measurement, super resolution microscopy and mass spectrometry imaging have been developed and employed in subcellular organelle studies to understand intercellular communication.[3] Among these techniques, amperometry coupled with small probes provides high spatiotemporal resolution and sensitivity while enabling direct quantification of electroactive transmitters and release dynamics.

With a carbon fiber microelectrode (CFME) or nanoelectrode (CFNE) in close vicinity to the cell surface, single cell amperometry (SCA) enables the quantification of the number of molecules ($N_{molecules}$) released and the dynamic information on single cells by analyzing the current transients resulted from the oxidation of transmitters expelled from single vesicles.[4] With a CFNE pierced into the cytoplasm, another technique called IVIEC was developed that allows the quantification of the $N_{molecules}$ originally stored inside single intracellular vesicles.[5] Then the fraction of release can be quantified by dividing the number of transmitters released over the vesicular content, and one of the main modes of exocytosis-partial release has been validated.[6] These studies at single-cell and subcellular levels with CFME and CFNE have significantly advanced the understanding of exocytosis and neurotransmission.

With CFME/CFNE, we generally obtain the average of $N_{molecules}$ and release kinetics of all the vesicles involved. The concentration of intravesicular chemical messengers is another key regulator that affects neurotransmission. In most of the present research, vesicle size and content have been studied separately, and the sizing relied on imaging techniques such as TEM (transmission electron microscopy) or NTA (nanoparticle tracking analysis).[7] Recently, Zhang et al. quantified catecholamine concentrations of isolated vesicles by combining resistive pulse measurements with glass nanopipettes and VIEC measurement with CFMEs, and the mechanism of vesicle maturation process was revealed by comparing the concentrations between non-DCVs and DCVs.[8] In 1997, Albillos et al. integrated cell-attached capacitance measurements with electrochemical detection by inserting a CFME into a patch pipette to estimate catecholamine concentration of single intracellular vesicles.[9] They showed that in single chromaffin cells all vesicles contain approximately the same concentration of catecholamine, though obvious morphological changes of cells were observed after CFMEs insertion. In 1998, Kozminski et al. used fast scan-rate cyclic voltammetry (FSCV) to show that the concentration of electroactive transmitters released to extracellular space during exocytosis of PC12 cells is relatively constant after exposure to L-DOPA.[10] Yet, new methodology is required for non-invasive quantification of single vesicular catecholamine concentrations in the intra-

[*] Dr. K. Hu,[+] K. L. Le Vo,[+] Dr. A. Hatamie, Prof. A. G. Ewing
Department of Chemistry and Molecular Biology
University of Gothenburg
Kemivägen 10, 41296 Gothenburg (Sweden)
E-mail: andrewe@chem.gu.se

[+] These authors contributed equally to this work.

Supporting information and the ORCID identification number(s) for the author(s) of this article can be found under: https://doi.org/10.1002/anie.202113406.

cellular environment. And investigations regarding the effects of drugs exposure on vesicular structure are still incomplete.

CNPs fabricated by chemical vapor deposition (CVD) of carbon into pre-pulled glasses have been applied into electrochemical detection of catecholamine.[11] Open CNPs are applicable to count single entities of liposomes and quantify intravesicular content simultaneously.[11b] Cavity CNPs have been employed in the measurement of exogenous dopamine in mouse-brain slices with FSCV showing high sensitivity and temporal resolution.[11d] Our previous work with isolated vesicles has shown that vesicular content can be correlated with vesicle size using open CNPs.[12] In this work, the orifice size was further decreased below 100 nm, thus, intracellular vesicles that can be translocated through pipette orifice were constrained between 50 and 100 nm radius. Based on the narrowed distribution of vesicular content and sizes achieved with 100 nm open CNPs, reliable information regarding catecholamine concentrations was obtained. We also explored the feasibility of this method in the mechanistic study of L-DOPA in exocytosis regulation. As a precursor of catecholamines, L-DOPA has been used in the clinical treatment of Parkinson's disease, an ailment that results in the death of dopaminergic neurons.[13] With open CNPs, the alterations of vesicular structure, catecholamine molecular number and concentration after exposure to L-DOPA were determined simultaneously.

A schematic of IVIEC measurement with open CNPs is presented in Figure 1 A (upper). Intracellular vesicles that are small enough to fit diffuse through the pipette orifice and expel their content onto the inner wall carbon surface. The resultant current transients correspond to the oxidation of messenger molecules from each vesicle and are recorded as single spikes. The tip of the CNP was used to penetrate through the cell membrane quite smoothly without any vibration in the base line, as shown in the representative amperometric traces in Figure 1 B, suggesting minimized invasion to cell membrane and intracellular environment. It

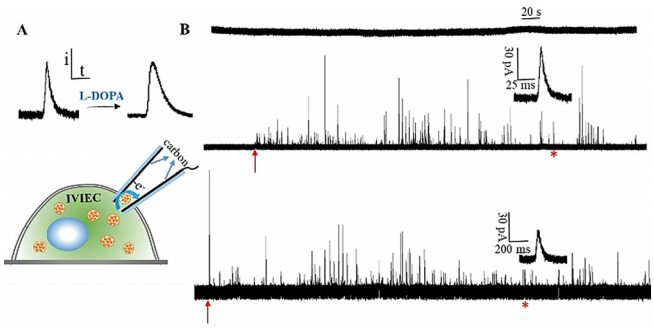

Figure 1. A) IVIEC measurement with open CNPs and shape transformation of single spikes after cell exposure to L-DOPA. B) Representative amperometric traces of 50 and 100 nm open CNPs obtained from L-DOPA treated and non-treated chromaffin cells at 700 mV vs. Ag/AgCl. (From top to bottom, amperometric traces obtained with 50, 100 nm CNPs for the control cells and 100 nm CNPs for L-DOPA-exposed cells; the inset shows an amplification of the spike labelled with the red asterisk; The red arrows indicate the moment CNPs were inserted into the cytoplasm, the recording was stopped when no more spikes were observed.)

appears that the carbon layer (about 10-nm) at the orifice of CNPs is too thin for vesicles to effectively adsorb and electroporate. No spikes were observed with a 50-nm CNPs, whereas spikes were observed with 100-nm CNPs suggesting that vesicles with radius between 50 and 100 nm opened on the inner carbon surface of CNP electrodes. Representative scanning electron microscopy (SEM) images of open CNPs are shown in Figure S1. These are consistent with previous EM images reported for intracellular vesicles, but distinguished from the electrochemical measurements of isolated vesicles as no vesicles below 100 nm radius were detected.[8,9,12] This indicates that vesicles, especially those with smaller size, might burst during isolation resulting from mechanical stimulation. An in situ intracellular evaluation with small open CNPs allows a comprehensive and discriminated mapping of intracellular vesicles by grouping them according to vesicle size. After cells are treated with L-DOPA, the intensity of current transients does not vary significantly, whereas the time duration increases significantly, as indicated by the representative amperometric traces and spikes labeled with the red asterisk.

Nine cells were examined under each condition. The average numbers of vesicles that enter the CNP and burst are 66 and 45 for the control cells and L-DOPA-exposed cells, respectively. The distributions of vesicular content obtained with 100 nm CNPs are shown in Figure 2 A. Vesicles with content of 1.0×10^6 account for the largest percentage of the vesicles below 100 nm, and that ratio decreases as vesicular content increases. For the control, vesicles with a content below 1.0×10^6 make up 68 % of the total vesicles while for the L-DOPA-exposed cells, the ratio of vesicles with larger content increases. After L-DOPA incubation, vesicles with the contents of 1.0×10^6 and 2.0×10^6 together account for 68 %. Thus, the distributions of both vesicular size and content were narrowed in a smaller range with 100 nm CNPs. The averages of vesicular content are presented in Figure 2 B, 582 800 for the control cells and 1323 000 for the L-DOPA-exposed cells., Vesicles below 60 nm make up very small ratio of the vesicles below 100 nm,[9] according to the equation $C = 3N_{molecules}/4N_A\times\pi\times r^3$ (C is catecholamine concentration, N_A is Avogadro's number and r is vesicle radius), based on the size range of 60 to 100 nm, we can derive the concentrations of catecholamine as 0.23–1.1 M for control cells. It should be noted that vesicle size increases after incubation with L-DOPA, and the largest detectable size is still 100 nm, which was controlled by pipette orifice. However, the smallest vesicles will be larger than 60 nm, and based on TEM imaging from a previous report, average vesicle size increases to 1.34 times of the original size after L-DOPA exposure.[14] Then the smallest size increases to 80.4 nm, and single vesicular catecholamine concentrations are calculated as 0.53 to 1.0 M after L-DOPA treatment. Compared with the control cells, these concentrations didn't show noticeable changes. This supports the idea that vesicles swell as more catecholamines are loaded into them, thus maintaining a constant osmolarity to avoid vesicle rupturing.[14] During this process, membrane lipids would experience a quick reorganization to be prepared for the expansion, suggesting a critical role of lipids in exocytosis regulation, as revealed by recent works.[15]

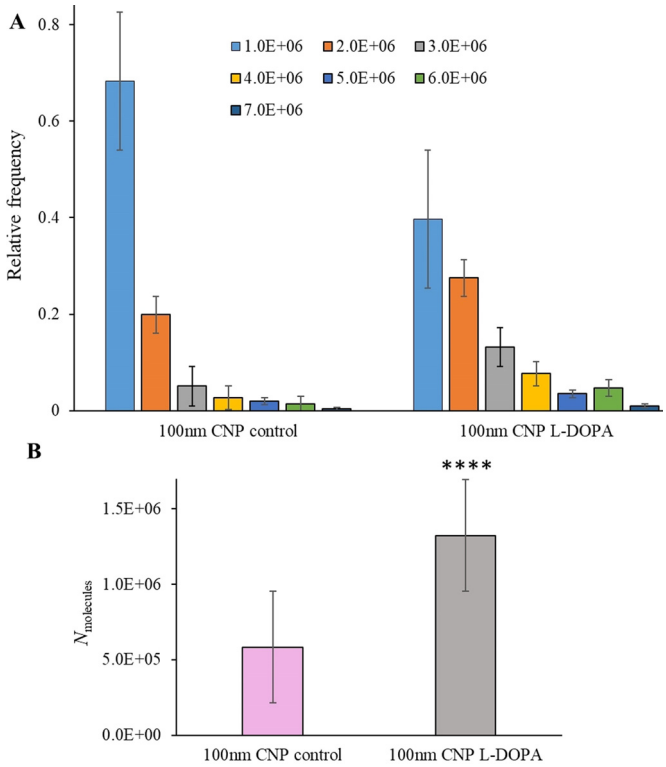

Figure 2. A) Normalized frequency histograms of vesicular content obtained from L-DOPA treated and non-treated chromaffin cells with 100 nm radius open CNPs. B) The averages of vesicular content obtained from L-DOPA-treated and non-treated chromaffin cells with 100 nm open CNPs. (Collected from 3 isolations of chromaffin cells; 9 cells were examined under each condition; 593 and 403 spikes for the control cells and L-DOPA-exposed cells, respectively. The value marked with **** are statistically different with $p < 0.0001$ versus the control (unpaired t test).)

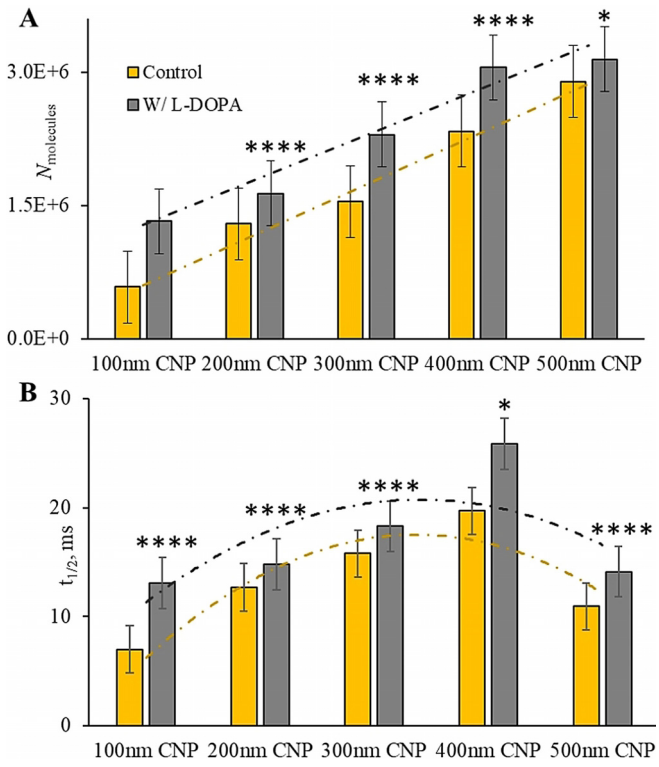

Figure 3. Histograms of A) vesicular content and B) release kinetics of the control cells and L-DOPA-exposed chromaffin cells derived from different-sized open CNPs with linear trend lines (A) and second-order polynomial trend lines (B), respectively. (Collected from 7 isolations of chromaffin cells, these results are based on the distributions presented in Figure S4. The values marked with **** and * are statistically different with $p < 0.0001$ and $P < 0.05$ versus the control, respectively (unpaired t test).)

We then employed open CNPs with radius of 200, 300, 400 and 500 nm in IVIEC measurements of L-DOPA-treated and non-treated chromaffin cells to investigate the effect of L-DOPA on vesicular content and release dynamics correlated with vesicle size. Orifice blocking was not observed for smaller CNPs below 400 nm while for 500 nm CNPs this occurs occasionally. The smaller and sharper CNPs penetrate through the cell membrane more smoothly compared with those that are larger. Different-sized vesicle populations were detected and differentiated. The normalized frequency histograms of intracellular vesicular content of control cells and L-DOPA-exposed chromaffin cells obtained with different-sized open CNPs are shown in Figure S4. The relative frequency was calculated by dividing the number of vesicles with a specific range of $N_{molecules}$ by the overall number of detected vesicles with the same size CNPs. Average results for vesicular content and release kinetics are presented in Figure 3 A and 3 B. All vesicles smaller than the orifice size can enter into and burst on the carbon surface. As the orifice size of CNPs increases, the detectable size range changes and increasingly larger vesicles are included, thus the new distribution brought by new size range changes the average. Our data show the average content of different vesicle populations obtained with different-sized CNPs increases with orifice size. Therefore, we conclude that for both L-DOPA-exposed and control cells, vesicular content increases with vesicle size, and this is in agreement with the idea that variation of catecholamine concentration between different-sized vesicles is small. A greater amount of catecholamine was produced after cell incubation with L-DOPA. The corresponding trend lines showing similar trend but obviously different amplitudes between the control and the treatment are presented in Figure 3 A and 3 B. Release kinetics shown in Figure 3 B are slower for L-DOPA-exposed cells. For both L-DOPA-loaded and control cells, the release rates of chemical messengers changed with vesicular dense core sizes,[12] demonstrating that after L-DOPA treatment dense core size increases accordingly and it still correlates with the release kinetics. This direct connection also applies for other vesicles with similar molecular machinery and can clearly explain the differences of release kinetics among synaptic vesicles, dense core vesicles and insulin granules, [16] which will facilitate the understanding of exocytosis of other systems. And, we can conclude that small alterations in dense core size occur, and overall vesicular size and catecholamine molecular number and concentration after L-DOPA treatment can be obtained simultaneously with open CNPs.

The data are best explained by catecholamines being mainly loaded into the halo part of LDCVs with short term

incubation of L-DOPA and a very small amount of catecholamine are loaded into the dense core.[17] However, this small number of catecholamines could alter the structure of the dense core, as indicated by the increase of the release rates. The dense core matrix is composed of chromogranins carrying anions stabilized by catecholamine cations.[2a] Then we can infer an increase of dense core size as a result of the addition of extra catecholamine cations after exposure to L-DOPA that interrupted the original electrostatic balance, as shown as a hypothesis in Figure 4. The dense core matrix could then

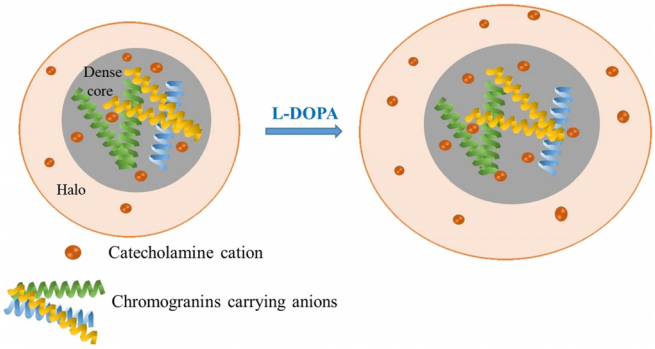

Figure 4. Underlying mechanism of vesicular structure transformation with enlarged dense core (owing to the increase of electrostatic interactions between catecholamine cations and chromogranins carrying anions) and overall vesicular size after cell exposure to L-DOPA.

expand due to the increase of electrostatic-interactions based on the physics of polyelectrolytes containing long chains of anionic moieties (here, chromogranins) condensed by a mixture of bulky cations (here, mainly catecholamines).[2a,18] However, previous TEM imaging showed that the dense core size didn't have obvious increase after L-DOPA treatment.[14,19] With amperometric measurement at open CNPs, we correlated the size of dense core with release rate in our previous work with isolated vesicles and in this work with intracellular vesicles after exposure to L-DOPA.[12] Electrochemical results showed more obvious alterations suggesting that the release kinetics were slowed down. One possibility is that after L-DOPA treatment the small change of dense core size was not easily observed with TEM imaging while the release kinetics is more sensitive to the structural change, and even slight variation can be identified.

In conclusion, direct and distinct mapping of intracellular vesicles was achieved by controlling the orifice sizes of open CNPs used for electrochemical measurements. IVIEC measurements with 100 nm open CNPs enabled the calculation of a range for intravesicular catecholamine concentration by limiting the detectable radius between 50 and 100 nm and narrowing the distribution of vesicular content. This is a significant advancement in the quantification of catecholamine concentrations with relatively noninvasive intracellular measurement of nanotips. We have shown that after exposure to L-DOPA, intravesicular catecholamine concentration is essentially identical to that for control, whereas both vesicular size and content increases. This also indirectly indicates that lipids play a fundamental role in exocytosis regulation. In addition, by use of CNPs with different pore size, we found that the micro structural change and the alteration of mutual interactions between the aggregated proteins and the transmitters in the vesicular dense core after drug exposure can be recognized by the variation of the release kinetics. This method with open CNPs with varied orifice size can be used for mechanistic investigations of pharmaceuticals in exocytotic regulation at the single-cell level and also in small living organisms.

Acknowledgements

We acknowledge funding from the European Research Council (ERC Advanced Grant Project No 787534 Nano-BioNext), Knut and Alice Wallenberg Foundation, and the Swedish Research Council (VR Grant No 2017–04366). We thank Dr. E. Ranjbari for SEM imaging of CNPs.

Conflict of Interest

The authors declare no conflict of interest.

Keywords: exocytosis · IVIEC · L-DOPA · open carbon nanopipettes · single vesicular catecholamine concentration

[1] a) J. H. Phillips, *Neuroscience* **1982**, *7*, 1595–1609; b) F. T. Horrigan, R. J. Bookman, *Neuron* **1994**, *13*, 1119–1129; c) W. B. Huttner, H. H. Gerdes, P. Rosa, *Trends Biochem. Sci.* **1991**, *16*, 27–30.
[2] a) A. Oleinick, R. Hu, B. Ren, Z.-Q. Tian, I. Svir, C. Amatore, *J. Electrochem. Soc.* **2016**, *163*, H3014–H3024; b) J. Yao, J. D. Erickson, L. B. Hersh, *Traffic* **2004**, *5*, 1006–1016.
[3] a) K. T. Kawagoe, J. A. Jankowski, R. M. Wightman, *Anal. Chem.* **1991**, *63*, 1589–1594; b) S. S. Rubakhin, R. W. Garden, R. R. Fuller, J. V. Sweedler, *Nat. Biotechnol.* **2000**, *18*, 172–175; c) K. I. Willig, S. O. Rizzoli, V. Westphal, R. Jahn, S. W. Hell, *Nature* **2006**, *440*, 935–939.
[4] a) R. M. Wightman, J. A. Jankowski, R. T. Kennedy, K. T. Kawagoe, T. J. Schroeder, D. J. Leszczyszyn, J. A. Near, E. J. Diliberto, O. H. Viveros, *Proc. Natl. Acad. Sci. USA* **1991**, *88*, 10754–10758; b) C. Gu, X. Zhang, A. G. Ewing, *Anal. Chem.* **2020**, *92*, 10268–10273.
[5] X. Li, S. Majdi, J. Dunevall, H. Fathali, A. G. Ewing, *Angew. Chem. Int. Ed.* **2015**, *54*, 11978–11982; *Angew. Chem.* **2015**, *127*, 12146–12150.
[6] N. T. N. Phan, X. Li, A. G. Ewing, *Nat. Rev. Chem.* **2017**, *1*, 48.
[7] a) J. Dunevall, H. Fathali, N. Najafinobar, J. Lovric, J. Wigström, A. S. Cans, A. G. Ewing, *J. Am. Chem. Soc.* **2015**, *137*, 4344–4346; b) L. Ren, A. Oleinick, I. Svir, C. Amatore, A. G. Ewing, *Angew. Chem. Int. Ed.* **2020**, *59*, 3083–3087; *Angew. Chem.* **2020**, *132*, 3107–3111.
[8] X. W. Zhang, A. Hatamie, A. G. Ewing, *J. Am. Chem. Soc.* **2020**, *142*, 4093–4097.
[9] A. Albillos, G. Dernick, H. Horstmann, W. Almers, G. Alvarez de Toledo, M. Lindau, *Nature* **1997**, *389*, 509–512.
[10] K. D. Kozminski, D. A. Gutman, V. Davila, D. Sulzer, A. G. Ewing, *Anal. Chem.* **1998**, *70*, 3123–3130.
[11] a) R. Singhal, S. Bhattacharyya, Z. Orynbayeva, E. Vitol, G. Friedman, Y. Gogotsi, *Nanotechnology* **2010**, *21*, 015304; b) R. Pan, K. Hu, D. Jiang, U. Samuni, M. V. Mirkin, *J. Am. Chem. Soc.* **2019**, *141*, 19555–19559; c) K. Hu, D. Wang, M. Zhou, J. H.

Bae, Y. Yu, H. Xin, M. V. Mirkin, *Anal. Chem.* **2019**, *91*, 12935 – 12941; d) C. Yang, K. Hu, D. Wang, Y. Zubi, S. T. Lee, P. Puthongkham, M. V. Mirkin, B. J. Venton, *Anal. Chem.* **2019**, *91*, 4618 – 4624.
[12] K. Hu, R. Jia, A. Hatamie, K. L. V. Long, M. V. Mirkin, A. G. Ewing, *J. Am. Chem. Soc.* **2020**, *142*, 16910 – 16914.
[13] G. C. Cotzias, P. S. Papavasiliou, R. Gellene, *N. Engl. J. Med.* **1969**, *280*, 337 – 345.
[14] T. L. Colliver, S. J. Pyott, M. Achalabun, A. G. Ewing, *J. Neurosci.* **2000**, *20*, 5276 – 5282.
[15] a) M. Aref, E. Ranjbari, A. Romiani, A. G. Ewing, *Chem. Sci.* **2020**, *11*, 11869 – 11876; b) M. R. Ammar, N. Kassas, S. Chasserot-Golaz, M. F. Bader, N. Vitale, *Front. Endocrinol. (Lausanne)* **2013**, *4*, 1 – 6.
[16] A. J. B. Kreutzberger, V. Kiessling, C. Stroupe, B. Liang, J. Preobraschenski, M. Ganzella, M. A. B. Kreutzberger, R. Nakamoto, R. Jahn, J. D. Castle, L. K. Tamm, *Nat. Commun.* **2019**, *10*, 3904.
[17] J. Lovrić, J. Dunevall, A. Larsson, L. Ren, S. Andersson, A. Meibom, P. Malmberg, M. E. Kurczy, A. G. Ewing, *ACS Nano* **2017**, *11*, 3446 – 3455.
[18] J. Wittmer, A. Johner, J. F. Joanny, *J. Phys. II* **1995**, *5*, 635 – 654.
[19] D. M. Omiatek, Y. Dong, M. L. Heien, A. G. Ewing, *ACS Chem. Neurosci.* **2010**, *1*, 234 – 245.

Manuscript received: October 3, 2021
Accepted manuscript online: November 3, 2021
Version of record online: November 23, 2021